GEOPHYSICAL RESEARCH LETTERS, VOL. 22, NO. 16, PAGES 2127-2130, AUGUST 15, 1995

Runaway electrons as a source of Red Sprites in the mesosphere

Timothy F. Bell, Victor P. Pasko and Umran S. Inan
STAR Laboratory, Stanford University, Stanford, California

Abstract. Large quasi-electrostatic (QE) fields above thunderclouds [*Pasko et al.*, 1995] produce an upward traveling beam of $\sim$1 MeV runaway electrons which may contribute to the production of optical emissions above thunderclouds referred to as Red Sprites. Results of a one dimensional computer simulation model suggest that the runaway electrons can produce optical emissions similar in intensity and spectra to those observed in Red Sprites, but only for large QE fields produced by positive CG discharges lowering 250 C or more to ground from an altitude of at least 10 km. Differences in predicted optical spectra from that of other mechanisms suggest that the runaway electron mechanism can be readily tested by high resolution spectral measurements of Red Sprites.

Introduction

Luminous glows, also known as 'upward discharges', following positive cloud-to-ground (CG) lightning discharges and occurring at altitudes ranging from cloud-tops to as high as 90 km, have been detected by imaging systems on the ground [*Franz et al.*, 1990; *Lyons*, 1994], on the Space Shuttle [*Boeck et al.*, 1992], and on aircraft [*Sentman et al.*, 1995; *Wescott et al.*, 1995].

The Red Sprite type of upward discharge is most common with sharp features and vertical structure, with response primarily in the red region of the spectrum, exhibiting short ($\sim$ 1 ms) duration, and generally detached from the cloud-tops but extending to as high as 95 km altitude [*Sentman et al.*, 1995].

Recently *Pasko et al.* [1995; hereafter referred to as I] proposed that Red Sprites are produced by the heating of mesospheric electrons by large quasi-electrostatic (QE) thundercloud fields. These QE fields appear following a positive CG lightning discharge, and their duration at any altitude is controlled by the local relaxation time of the E field [I]. This new mechanism accounts for many of the observed aspects of these discharges but does not appear to explain emissions below 60 km which some Red Sprites exhibit.

In the present work, we explore the possibility that high energy (20 keV-20 MeV) runaway electrons (REL) may be involved in producing the low altitude portion of the optical output associated with Red Sprites (Figure 1a). We examine this question within the context of the QE model [I].

The subject of REL directly over thunderstorm cells has been addressed by *McCarthy and Parks* [1992], *Gurevich et al.* [1992,1994] and *Roussel-Dupre et al.* [1994] (see also references cited therein). These papers have shown that secondary cosmic ray electrons of energy $\sim$1 MeV can become REL whenever the local E field exceeds the threshold field $E_t = \frac{4\pi N_m Z e^3 a}{mc^2}$, where N_m is the number density of air molecules, $Z \simeq 14.5$, $a \simeq 11$, m and e are the electron rest mass and charge, respectively, and c is the velocity of light [*Gurevich et al.*, 1994]. The main energy loss for the REL occurs from inelastic collisions with O_2 and N_2 molecules, resulting in optical excitation of the neutrals, and subsequent optical emissions may result.

Paper number 95GL02239
0094-8534/95/95GL-02239$03.00

Model

For simplicity, we consider a 1-D model for the REL, but base the parameters for this model on 2-D calculations of the QE field carried out through the procedure outlined in [I].

2-D Model of the QE Field

Figure 1b, c, d shows 2-D electric field calculations for the case in which the initial thundercloud charge consists of $\pm$300 C at altitudes of 10 km and 5 km respectively. Each total dipole charge $\pm Q$ is represented as a spatially distributed charge density $\rho(\vec{r}, t)$ which is assumed to have a Gaussian spatial distribution ($e^{-((z-z_o)^2+r^2)/a_o^2}$) with a_o = 3 km and related to the total source charge Q as $Q(t) = \int \rho_s(\vec{r}, t) dV$ [I]. The ground is assumed to be a perfect conductor. The separated dipole charges are assumed to form over a time $\tau_f >$ 100 s, and subsequently the positive half of the dipole charge is discharged to ground with a time constant τ_s. In each case, as the charges accumulate, high altitude regions where τ_f is greater than the local electric relaxation time (σ/ϵ_o) are shielded from the E fields of the thundercloud charges by induced space charge at lower altitudes. When the positive charge is discharged to ground, an E field appears at all altitudes well above the shielding space charge. Physically, the removal of $+Q$ is equivalent to placing $-Q$ at the same point in space. The initial E field above the space charge is then approximately the free space E field due to the newly placed $-Q$ and its image in the ground plane. Thus the important physics of the system concerns only the magnitude and altitude of the removed charge and is essentially independent of all other charges present in the thundercloud.

Figure 1b shows the dependence of the post-discharge E field upon the initial altitude of the thundercloud dipole charges (3-6 km, 4-8 km, and 5-10 km, for negative and positive charges, respectively). Figure 1c shows the dependence of the post-discharge E field on the initial atmospheric conductivity profile. This profile determines the local relaxation time of the QE fields, as well as the spatial structure of the space charge accumulated in and around the thundercloud during the charge separation process. The profile $\sigma_D = 5 \times 10^{-14}\ e^{z/6\text{km}}$ mho/m is taken from *Dejnakarintra and Park* [1974]; the profile $\sigma_L = 6 \times 10^{-13}\ e^{z/11\text{km}}$ mho/m is taken from *Holzworth et al.* [1985].

Figure 1d shows a 2-D plot of the post-discharge ratio $\delta_o = E/E_t$ in a cylindrically symmetric coordinate system in which the z axis represents altitude and the radial coordinate r represents horizontal distance from the z axis. The dipole charge distributions are centered on the z axis as described above. The plot displays a 2-D cross section which passes through the z axis. Note that REL ($\delta_o > 1$) can occur within a large conical volume of space above the thundercloud from which the positive CG discharge occured, and that δ_o increases with altitude. The avalanche process associated with the energetic REL is controlled predominantly by δ_o [*Gurevich et al.*, 1992,1994; *Roussel-Dupre et al.*, 1994], which determines the percentage of low energy secondary electrons produced by the energetic REL which become REL themselves after being accelerated by the QE field.

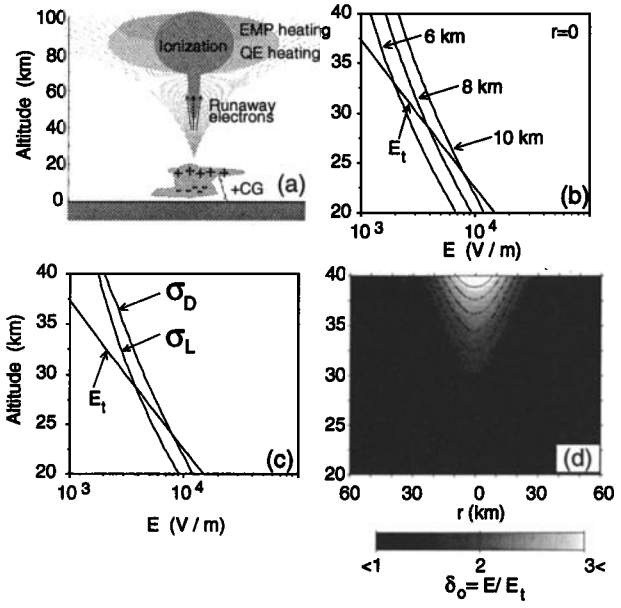

Figure 1.(a) Illustration of three possible mechanisms for producing Red Sprites: electron heating by the electromagnetic pulse (EMP) [*Taranenko et al.*, 1993], and/or the QE field [I], and/or optical excitation by runaway MeV electrons. (b) Dependence of post-discharge E upon initial altitude of thundercloud positive charge above ground. The threshold field E_t is also shown. (c) Dependence of E upon ambient conductivity profile. (d) Two dimensional cross sectional plot of the ratio $\delta_o = E/E_t$ above the thundercloud.

1-D Model of Runaway Electrons

Runaway electrons and ion spacecharge. On the z axis directly over the thundercloud charge where $\vec{E}$ is vertical, the transport equation for the REL can be written as:

$$\frac{\partial N_R}{\partial t} + v_R \frac{\partial N_R}{\partial z} = \frac{N_R}{\tau_i} + S_o(z) \tag{1}$$

where N_R is the number density of the REL, $v_R \approx c$ is their mean velocity along the z axis, τ_i is the ionization time constant, S_o is the local source function for energetic cosmic ray secondary electrons, c is the speed of light and where for simplicity the Earth's magnetic field is assumed vertical. At an altitude of $\sim$10 km , $S_o \cong 10^{-5}$/cm^3-sec and is proportional to the atmospheric density at higher altitudes [*McCarthy and Parks*, 1992]. The first term on the r.h.s. of (1) represents the avalanche effect in which each REL creates new REL through impact ionization. The explicit dependence of τ_i on δ_o can be obtained from *Roussel-Dupre et al.* [Table II, 1994]: $\tau_i = \left[\frac{18}{\delta_o}\right]^{1.5} \lambda(z)$ ns for $1.5 \le \delta_o \le 5$, and $\tau_i = \left[\frac{13.7}{\delta_o}\right]^{1.9} \lambda(z)$ ns for $5 \le \delta_o$, where $\lambda(z) = 1.53 \times 10^{19}$ cm^{-3} / $N_m(z)$, and where for simplicity we assume $\tau_i = \infty$ for $\delta_o < 1.5$.

Almost all the REL are produced by impact ionization of neutrals, and the resulting ions are left behind as positive space charge. The transport equation for these ions is:

$$\frac{\partial N_{is}}{\partial t} = \frac{N_R}{\tau_i} + S_o(z) \tag{2}$$

where N_{is} is the number density of the space charge ions.

Secondary electrons. The REL also produce low energy secondary electrons which do not become runaways but instead thermalize through collisions with the neutrals. This effect produces a local increase in ionization, but no uncompensated space charge.

The rate of production by the energetic REL of low energy secondary electrons within an energy range $d\varepsilon$ centered around ε can be found from the relation:

$$\frac{\partial N_s(\varepsilon)}{\partial t} = S_s(\varepsilon) \cong v_R N_R \sum_j \frac{\sigma_i^j(\varepsilon') N_j d\varepsilon}{\varepsilon_{oj}(\varepsilon/\varepsilon_{oj}+1)^{2.1}} \tag{3}$$

where $\sigma_i^j(\varepsilon)$ is the total ionization cross section for species j, ε' is the mean energy of the REL, N_j is the number density of species j, and $\varepsilon_{oj} = 13$ eV for N_2, and $\varepsilon_{oj} = 17.4$ eV for O_2 [*Opal et al.*, 1972]. For simplicity we choose $\sigma_i(\varepsilon) = 2.3 \times 10^{-18}$ cm^2 for both N_2 and O_2. This value is consistent with the energy loss due to dynamic friction for the REL [e.g., *Gurevich*, 1992] and the electron-impact ionization cross section for N_2 extrapolated from 300 KeV energy [*Kim*, 1975; *Kim and Rudd*, 1994].

The low energy secondaries are rapidly thermalized through inelastic collisions with the neutrals and their differential number density within the energy range $d\varepsilon$ about ε has the equilibrium value [*Gurevich*, 1978]: $N_s(\varepsilon) \cong \frac{S_s(\varepsilon)}{\nu_{in}(\varepsilon)}$ where $\nu_{in}(\varepsilon) = v_s \sum_j \sigma_{in}^j(\varepsilon) N_j$ is the total frequency of inelastic collisions, v_s is the velocity of the secondary electrons of energy ε, and $\sigma_{in}^j(\varepsilon)$ is the cross section for inelastic collisions with species j. The differential omnidirectional flux $I(\varepsilon)$ associated with the low energy secondary electrons of energy ε and velocity v_s is:

$$I(\varepsilon)d\varepsilon = N_s(\varepsilon)v_s = \frac{S_s(\varepsilon)}{\sum_j \sigma_{in}^j(\varepsilon) N_j} \tag{4}$$

Optical emissions. The flux of low energy secondary electrons will excite the neutral species through impact excitation, leading to optical emissions. The excitation rate of a given energy state k for a particular species j has the value:

$$R_k = N_j \int \sigma_k(\varepsilon) I(\varepsilon) d\varepsilon, \tag{5}$$

where $\sigma_k(\varepsilon)$ is the cross section for excitation of state k. The intensity of each optical line in Rayleighs is given by the expression [*Chamberlain*, 1978]:

$$I_k = 10^{-6} \int A_k n_k dz, \tag{6}$$

where n_k is the number density of excited particles in state k, A_k is the radiation transition rate, and the integral is taken along the line of sight. The quantity n_k is governed by the relation [*Sipler and Biondi*, 1972]:

$$\frac{\partial n_k}{\partial t} = -\frac{n_k}{\tau_k} + \sum_m n_m A_m + R_k \tag{7}$$

where $\tau_k = [A_k + \alpha_1 N_{N_2} + \alpha_2 N_{O_2}]^{-1}$ is the total lifetime of state k, α_1 and α_2 are the quenching rates due to collisions with N_2 and O_2 molecules, respectively, N_{N_2} and N_{O_2} are the number densities of N_2 and O_2 molecules respectively, and the sum over the terms $n_m A_m$ represents increases in n_k resulting from cascading from higher energy states.

We consider optical emissions from the 1st ($B^3\pi_g \rightarrow A^3\Sigma_\mu$) and 2nd ($C_3\pi_\mu \rightarrow B^3\pi_g$) positive bands of N_2, the Meinel and 1st negative bands of N_2^+, and the 1st negative band of O_2^+, for which the transition rates are 1.7×10^5/sec, 2×10^7/sec, 7×10^4/sec, 1.4×10^7/sec, and 8.5×10^5/sec respectively [*Valence-Jones*, 1974]. Quenching of the 1st positive band emissions occurs primarily through collisions with N_2 molecules, with $\alpha_1 = 10^{-11}$ cm^3/sec [*Valence-Jones*, 1974]. Quenching of the 2nd positive band occurs primarily through collisions with O_2 molecules with $\alpha_2 = 3 \times 10^{-10}$ cm^3/sec [*Valence-Jones*, 1974]. For quenching of the Meinel and 1st negative bands of N_2^+ we have $\alpha_1 = 5 \times 10^{-10}$ cm^3/sec and $\alpha_1 = 4 \times 10^{-10}$ cm^3/sec respectively, and for the 1st negative band of O_2^+ we have $\alpha_1 = 2 \times 10^{-10}$ cm^3/sec . The cross sections for excitation of the states $B^3\pi_g$ and $C_3\pi_\mu$, which are used in (7), are taken from *Rees* [1989, Figure A4.4]. The cross sections $\sigma_{in}(\varepsilon)$ used in (4) are also obtained from *Rees* [1989; Figure A4.1 and A4.2].

The production rate of ions N_j^+ in the excited state k is:

$$R_k = p_k v_R N_R N_j \sigma_i^j(\varepsilon') \quad (8)$$

where p_k is the branching ratio for state k. The branching ratios for the excited states $A^2\Pi_\mu$ and $B^2\Sigma_\mu^+$ of N_2^+ and $b^4\Sigma_g^-$ of O_2^+ (leading to emissions in the Meinel band and the 1st negative band of N_2^+, and the 1st negative band of O_2^+) have the respective values 0.39, 0.11, and 0.15 [*Rees*, 1989].

Electric field and conductivity. Another relationship used in our model is the 1-D divergence relationship for $\vec{E}$:

$$\frac{\partial E_z}{\partial z} = \frac{1}{\epsilon_o}[\rho_s(z,t) + \rho_c + eN_{is} - eN_R] \quad (9)$$

where ρ_s is the effective source charge distribution which reproduces the geometry of the E field obtained from 2-D calculations, and ρ_c is the conduction charge density related to E_z by the continuity equation:

$$\frac{\partial \rho_c}{\partial t} + \frac{\partial}{\partial z}[\sigma(z,t)E_z(z,t)] = 0 \quad (10)$$

where $\sigma(z,t)$ is the local conductivity which is calculated self-consistently. The ambient ion conductivity is assumed to be: $\sigma_D = 5 \times 10^{-14} e^{z/6\text{km}}$ mho/m [*Dejnakarintra and Park*, 1974]. At ionospheric altitudes, the electron component of σ is initially determined using a 'tenuous' model of the ambient ionospheric electron density [*Taranenko et al.*, 1993], and thereafter the electrons given by (3) are also included. The electron mobility is based on experimental data [*Davies*, 1983]. We neglect the effect of the geomagnetic field on σ since the plasma, even after minor heating, is highly collision dominated.

Equations (1), (2), (3), (9) and (10) are solved over the altitude range $0 \le z \le 90$ km. The E field in the system is assumed to be produced by a time varying charge ρ_s. The temporal boundary conditions for the system are $N_R(t=0) = 0$ and $\rho_s(t=0) = 0$. Initially the charge ρ_s is assumed to increase as $\rho_o(z)tanh(t/\tau_s)/tanh(1)$ where the characteristic discharge time τ_s is measured in msec and $\rho_o(z)$ is a given function obtained from 2-D calculations (e.g., Fig.1). For $t > \tau_s$, ρ_s=$\rho_o(z)$. The quantity $\rho_o(z)$ is chosen so that at $t = \tau_s$ the 1-D electric field profile $E(z)$ is identical to that predicted by the 2-D model [I] with $N_R \equiv 0$.

Results

Figure 2a shows N_R at four different altitudes as a function of time. At $t = 0$, $\rho_s = 0$ and $E = 0$. The runaway process starts before ρ_s reaches its final maximum value at $t = 1$ ms. N_R reaches its peak value at an altitude of 80 km at $t \sim 1$ ms and then decays. Above 80 km altitude the REL experience few collisions and escape upward. The burst of REL terminates at $t \sim 1.25$ ms at altitudes greater than 60 km because of E field relaxation. Since the relaxation time at 50 km altitude is longer, the REL process continues there past $t = 1.5$ ms. However for $t > 1.5$ ms the REL at 50 km altitude do not reach 60 km altitude because $E < E_t$ over most of the intervening space, and these electrons rapidly lose energy and thermalize above 50 km altitude. Thus the total duration of the burst of REL escaping upward is ~0.5 ms.

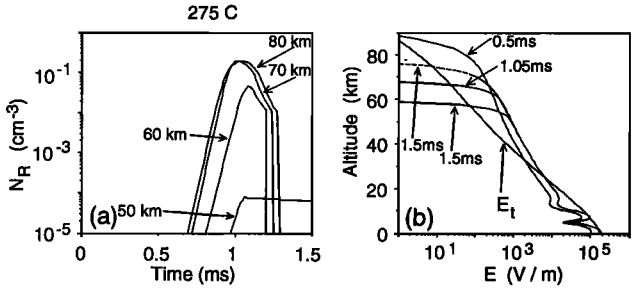

Figure 2. (a) The number density N_R of runaway electrons as a function of time at four altitudes; (b) the altitude distribution of thundercloud E field at selected instants of times following the positive CG lightning discharge. The dashed line shows E when $N_R \equiv 0$.

Figure 2b shows the altitude distribution of the E field in the system at selected instants of time (0.5, 1.05, and 1.5 ms). Relaxation of the E field with the assumption of no REL in the system (purely due to finite conductivity of the medium) is also shown for reference by the dashed line. One can see that the presence of REL can lead to a significant self consistent reduction of E.

Figure 3a shows, at $t = 1.05$ ms, the altitude profiles of N_R for five values of the effective thundercloud charge Q, and the altitude profiles of the space charge ions (N_{is}) and secondary electrons (N_{es}) for $Q = 275$ C. The quatities N_{is} and N_{es} are shown by dashed lines. The ambient number density profile of thermal electrons is also shown for reference. Clearly N_R is a sensitive function of Q. Both N_{is} and N_{es} peak near 60 km altitude with $N_{is} \sim 1$ cm^3 and $N_{es} \sim 10^3$ cm^{-3}. At altitudes above ~ 65 km, at t =1.05 ms, $E < E_t$, but the REL escape the system nevertheless because the atmosphere above ~ 60 km is not dense enough to stop them.

Figure 3b shows the optical intensity per unit volume of the 1st and 2nd positive bands of N_2, the Meinel and 1st negative bands of N_2^+, and the 1st negative band of O_2^+. This intensity, $A_k n_k$, forms the integrand of (6). The output was calculated using (3)-(7), and the steady state solutions for (9) were used since $\tau_k \ll 1$ msec. The two positive bands of N_2 dominate the spectrum up to ~80 km, above which the Meinel band of N_2^+ also becomes important.

Figure 3c gives the optical intensity per unit volume of the 1st positive band of N_2 produced by the REL. The five plots shown correspond to specific values of Q. It can be seen that the optical output depends very sensitively on Q. The same is true for all excited bands, but this is not shown for the sake of brevity.

Figure 3d shows the results for two different models of ambient ion conductivity. Lower values of N_R and corresponding optical

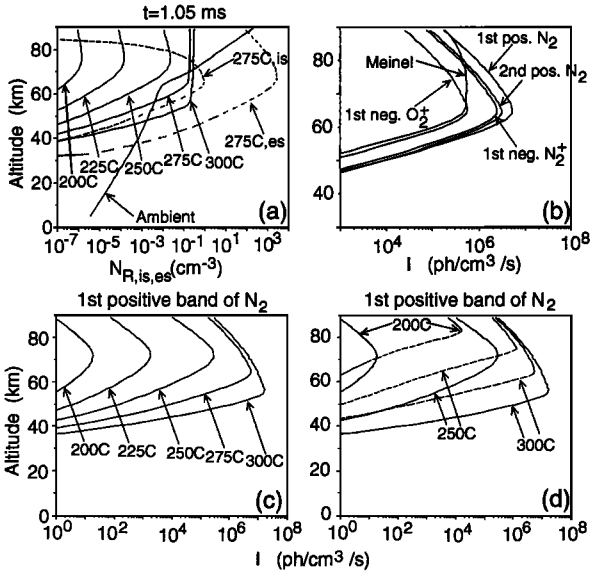

Figure 3. (a) The number density of runaway electrons (N_R), space charge positive ions (N_{is}), and secondary electrons (N_{es}) as a function of altitude for selected thundercloud charges; (b) The optical intensity profile of selected bands for N_2, N_2^+ and O_2^+ for a thundercloud charge of 275 C; (c) The optical intensity profile of the 1st positive band of N_2 for selected thundercloud charge values; (d) Altitude profile of optical intensity for two models of ambient ion conductivity and three values of Q.

emissions are obtained for the conductivity model σ_D [*Dejnakarintra and Park*, 1974] than for a low conductivity model σ_L similar to that measured experimentally by *Holzworth et al.* [1985]. Lower ambient σ at ionospheric altitudes corresponds to longer times of E field relaxation and leads to increased REL number density and optical output (up to 3 orders of magnitude at ~80 km altitude for 200C). On the other hand, the optical emissions for the two models are very similar for $Q > 250$C, because the REL effects control the E field relaxation.

Observations [*Sentman et al.*, 1995] suggest that the typical diameter of a Red Sprite is ~10 km (~10^6 cm). Thus for this case, from (6), the horizontal scale of Figures 3b, c, d can be interpreted as the intensity in Rayleighs. Since typical intensities for Red Sprites are ~100 kR [*Sentman et al.*, 1995], the figures indicate that Q must be at least 250 C in order to reproduce the observed results.

Discussion

Observations indicate that the brightest region of a Red Sprite lies between 66 and 74 km and that some Red Sprites exhibit significant intensity at altitudes as low as 40-50 km [*Sentman et al.*, 1995].

As shown in Figure 3, the REL optical emissions tend to peak in the 55-70 km altitude range, and substantial intensity can be found at altitudes as low as 45 km. Thus the predictions of the REL model fit the observations reasonably well. In comparison with other mechanisms, we note that the predicted optical emissions for QE heating [I] and EMP heating [*Taranenko et al.*, 1993] peak at 80-95 km altitude and have no significant intensity below 60 km.

There are two other notable differences in the model predictions 1) the ratio R_{12} of intensity of the 1st positive band of N_2 to the 2nd positive band of N_2 is ~2 at all altitudes above 60 km for our REL model, while for the QE and EMP models R_{12} ~10 above 80 km altitude; and 2) in the REL model the intensity of the Meinel band of N_2^+ and the 2nd positive band of N_2 are roughly equal at 80 km altitude, while for the EMP mechanism the intensity of the Meinel band of N_2^+ is smaller than that of the 2nd positive band of N_2 by a factor of ~10^3. As a result of these differences, spectral analysis of Red Sprites will provide an important test of the three proposed generation mechanisms. In the event that all three mechanisms operate simultaneously to create Red Sprites, altitude profiles of spectral ratios could determine the regions dominated by each mechanism.

Acknowledgements. This work was supported by NASA under Grant NAGW-2871.

References

Boeck, W. L., O. H. Vaughan, Jr., R. Blakeslee, B. Vonnegut, and M. Brook, Lightning induced brightening in the airglow layer, *Geophys. Res. Lett., 19*, 99, 1992.

Chamberlain, J. W., *Physics of the aurora and airglow*, Academic Press, New York, 1961.

Davies, D. K., Measurements of swarm parameters in dry air, *Thearetical Notes*, Note 346, Westinghouse R and D Center, Pittsburg, May, 1983.

Dejnakarintra, M. and C. G. Parks, Lightning-induced electrical fields in the ionosphere, J. Geophys. Res., 79, 1903, 1974.

Franz, R. C. et al., Television image of a large upward electric discharge above a thunderstorm system, *Science, 249*, 48, 1990.

Gurevich, A. V., *Nonlinear Phenomena in the Ionosphere*, Springer-Verlag, New York, 1978.

Gurevich, A. V., G. M. Milikh, and R. A. Roussel-Dupre, Runaway electron mechanism of air breakdown and preconditioning during a thunderstorm, *Phys. Lett. A, 165*, 463, 1992.

Gurevich, A. V., G. M. Milikh, and R. A. Roussel-Dupre, Nonuniform runaway air-breakdown, *Phys. Lett. A, 187*, 197, 1994.

Kim, Y-K., Energy distribution of secondary electrons II: "Normalization and extrapolation of experimental data", *Radiation Research, 64*, 205, 1975.

Kim, Y-K., and M. E. Rudd, Binary-encounter-dipole model for electron-impact ionization, *Phys. Review A, 50*, 3954, 1994.

Lyons, W. A., Characteristics of luminous structures in the stratosphere above thunderstorms as imaged by low-light video, *Geophys. Res. Lett., 21*, 875, 1994.

McCarthy, M. P., and G. K. Parks, On the modulation of X Ray fluxes in thunderstorms, *J. Geophys. Res., 97*, 5857, 1992.

Opal, C. B., E. Beatty, and W. Peterson, Measurements of secondary electron spectra produced by electron impact ionization of a number of simple goses, *Atomic Data, 4*, 209, 1972.

Pasko, V. P., U. S. Inan, Y. N. Taranenko, and T. F. Bell, Heating, ionization and upward discharges in the mesosphere due to intense quasi-electrostatic thundercloud fields, *Geophys. Res. lett., 22*, 365, 1995.

Rees, M. H., *Physics and Chemistry of the upper atmosphere*, Cambridge University Press, New York, 1989.

Roussel-Dupre, R. A., A. V. Gurevich, T. Tunnell, and G. M. Milikh, Kenetic theory of runaway air breakdown, *Phys. Rev. E, 49*, 2257, 1994.

Sentman, D. D., E. M. Wescott, D. L. Osborne, D. L. Hampton, M. J. Heavner, Preliminary results from the Sprites94 campaign: Red Sprites, *Geophys. Res. Lett., 22*, 1205, 1995.

Sipler, D. P., and M. A. Biondi, Measurements of O(^{1}D) quenching rates in the F region, *J. Geophys. Res., 77*, 6202, 1972.

Taranenko, Y. N., U. S. Inan and T. F. Bell, The interaction with the lower ionosphere of electromagnetic pulses form lightning: excitation of optical emissions, *Geophys. Res. Lett., 20*, 2675, 1993.

Valence-Jones, A., *Aurora*, D. Reidel publishing Co., Dordrecht, 1974.

T. F. Bell, V. P. Pasko, and U. S. Inan, STAR Laboratory, Stanford University, Stanford, CA 94305-4055.

(Received: March 10, 1995; revised: June 22, 1995
accepted: June 28, 1995)